

Computational Investigation on Flow of Nanofluid past an Exponentially Stretching Surface using VHPM

D. Mahalakshmi and B. Vennila*

Abstract—The theory of nanoliquids has revealed several fundamental properties, including a significant increase in thermal conductivity over the base fluid. In this study, we analyzed the nanoliquids two-dimensional laminar boundary layer flow over an exponentially stretching surface. Suitable variables are applied to simplify the nonlinear partial differential equations (PDEs) into ordinary differential equations (ODEs). The resulting equations are analytically solved by using the variational homotopy perturbation method (VHPM), and the graphical representation obtained with the help of the expressions for momentum, temperature, and concentration are evaluated for specific estimates of the dimensionless parameters, specifically the Lewis number (Le), Brownian motion parameter (Nb), thermophoresis parameter (Nt), Prandtl number (Pr), of suction and injection parameters.

Index Terms— Brownian motion, $bvp4c$, Exponentially Stretching Surface, Nanoliquids, Thermophoresis

NOMENCLATURE

a	Stretching rate (S^{-1})
C	Concentration (kgm^{-3})
C_w	Fluid wall concentration (kgm^{-3})
C_∞	Ambient concentration (kgm^{-3})
C_{fx}	Skin friction coefficient (—)
D_B	Brownian diffusion coefficient ($m^2 s^{-1}$)
D_T	Thermophoretic diffusion coefficient ($m^2 s^{-1}$)
$f(\eta)$	Velocity similarity function (—)
$g(\eta)$	Temperature similarity function (—)
$h(\eta)$	Concentration similarity function (—)
ℓ	Characteristic of the surface length
Le	Lewis Number (—)
Nb	Brownian Motion parameter (—)
Nt	Thermophoresis parameter (—)
Nu_x	Nusselt number (—)
Pr	Prandtl number (—)
Sh_x	Sherwood number (—)
Re_x	Reynolds number (—)
v_w	Suction/injection parameter (—)
U_w	Velocity of the sheet ($m s^{-1}$)
u, v	Velocity components ($m s^{-1}$)
x, y	Cartesian coordinates (m)

δ	Suction and injection velocity
ϑ	Viscosity (Nsm^{-2})
ρ_{nf}	Density (kgm^{-3})
$(\rho c)_{np}$	heat capacitance of the nanoparticles ($J kg^{-1}K^{-1}$)
$(\rho c)_{nf}$	heat capacitance of the nanofluid ($J kg^{-1}K^{-1}$)
α	Thermal diffusivity ($m^2 s^{-1}$)
η	Similarity function (—)
ν	Kinematic viscosity ($m^2 s^{-1}$)

I. INTRODUCTION

Recently, nanoliquids have seen a surge in usage for various industrial applications. They have some nanomaterials in them. Water, engine oil, and ethylene glycol are common substances that have a low heat conduction capacity and so inhibit heat transfer. In contrast, metals such as copper and aluminium are very conductive to heat. Therefore, the conduction heat transfer (HT) in the fluid suspension is enhanced by the thermal conductivity of the solid particles. Choi and Eastman [1] presented the concept of nanoliquids. The convective flow of a viscous fluid over a plate that moves under the assumption of nanoparticles was studied by Jalili et al. [2]. Patil et al. [3] investigated the Williamson nanoliquid flow over a rough conical surface as a function of time-varying nonlinear convection. They have noticed that the distance between the nanoparticles and the wall enhanced the thermophoresis. The MHD pair-stress hybrid nanoliquid flow traverses through a porous medium with viscous dissipation, as scrutinized by Mahesh et al. [4]. Alzahrani et al. [5] found that the flow of hybrid nanofluid passes through a flat plate. The consequences of Soret and Dufour's convection flow of Maxwell hybrid nanofluid were examined by Rauf et al. [6].

Numerous stretching surfaces of varying geometries and stretching paces have been studied for their significance in fluid mechanics. The effects of significant nonlinear convection on a nanofluid's flow over a stretching sheet (SS) were investigated by Rawat et al. [7]. Verma et al. [8] performed the unsteady mixed convective nanoliquid flow through an expanded SS with porous medium. The three-dimensional Maxwell nanofluid flow through porous medium past a SS was inspected by Wang et al. [9]. The magnetohydrodynamics nanofluid flow over an exponentially SS was numerically investigated by Amjad et al. [10]. Jawad et al. [11] explored the convection of a Maxwell nanoliquid in a linear porous SS. The nonlinear SS of a Carreau nanofluid flow with thermal radiation was delved into by Alrehili [12]. Eswaramoorthi et al. [13] investigated the water-based nanoliquid flow over a heated SS.

Manuscript received April 5, 2023; revised March 3, 2024.

D Mahalakshmi is a Research Scholar in the Department of Mathematics, College of Engineering and Technology, SRM Institute of Science and Technology, SRM Nagar, Kattankulathur, Chengalpattu-603 203, Tamil Nadu, India (e-mail: md1094@srmist.edu.in)

B Vennila is an Associate Professor in the Department of Mathematics, College of Engineering and Technology, SRM Institute of Science and Technology, SRM Nagar, Kattankulathur, Chengalpattu-603 203, Tamil Nadu, India. (Corresponding author, Phone: +91-9445413186 email id: vennilab@srmist.edu.in).

The HT of the boundary layer flow past a SS has become a trending subject in fluid mechanics because of its numerous applications in advanced industry and technology, which are utilized in polymer extrusion materials, copper wire drawing, artificial fibres, hot rolling, etc. More recently, immense research in convective heat transfer nanoliquids has played a significant role in various industrial processes. Negi et al. [14] analyzed the flow of a nanoliquid over a SS at the stagnation point, where there is no surface mass flux. The mixed convection in nanoliquid flow over a porous medium was explored by Sedki [15]. He noticed that the rate of HT improved as the porous medium was reduced in thickness. The HT of viscoelastic nanoliquid flow over a SS was probed by Alrehili [16]. He discovered that larger Brownian diffusion parameters or smaller Lewis's parameters led to an immense rise in nanoparticle concentration. Saidulu and Reddy [17] performed the HT in micropolar flow along a SS. They observed that the concentration rises as the magnetic parameter rises. The HT of second-grade fluid flowing over a vertical Riga sheet was scrutinized by Shatanawi et al. [18]. They uncovered that an increase in the boundary layer's concentration reduced mass transfer due to thermophoresis. Guled et al. [19] inspected the HT effects of MHD flow with suction and injection over a SS. The HT of Casson nanoliquid flow past a 3D Riga plate was probed by Loganathan et al. [20]. Divya et al. [21] scrutinized the non-Fourier HT analysis through a Riga plate with a heat sink or source. They observed that the HT gradient rose with improved values of the suction or injection parameters. The mixed convection of Williamson nanoliquid flow with Cattaneo-Christov HT was explored by Eswaramoorthi et al. [22].

The goal of this research is to examine the influence of Brownian motion and thermophoresis on the HT when a nanoliquid flows in a laminar 2D boundary layer past an exponentially sized SS. Suitable variables are applied to simplify the nonlinear PDEs into ODEs. The resulting equations are analytically solved by using the Variational Homotopy Perturbation Method (VHPM) [23–26] and the graphical representation obtained with the help of MATLAB bvp4c. Graphs are utilized to examine the relationships between modifications in these crucial components and the resulting variations in the temperature, concentration, and velocity profiles. A few more cutting-edge research reports in fluid mechanics are seen in refs. [27–31].

II. BASIC FLOW THEORY

Let consider the steady 2D boundary layer flow of incompressible nanoliquid over an exponentially stretching sheet. Assumed that the sheet and its normal is taken from the axis of x and y in Cartesian coordinates. In the direction of x , the velocity of a SS is defined as $U_w = U_0 e^{(x/\ell)}$ at $y=0$. Where ℓ is a characteristic of the surface length, U_0 is the constant velocity characteristic of the surface. The governing system of equations representing the steady form as:

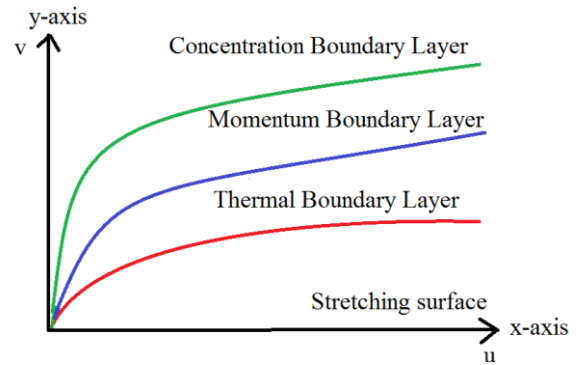


Figure 1: Flow model.

Continuity Equation:

$$\frac{\partial u}{\partial x} + \frac{\partial v}{\partial y} = 0 \tag{1}$$

Momentum Equation:

$$u \frac{\partial u}{\partial x} + v \frac{\partial v}{\partial y} = \nu_{nf} \frac{\partial^2 u}{\partial y^2} \tag{2}$$

Energy Equation:

$$u \frac{\partial T}{\partial x} + v \frac{\partial T}{\partial y} = \alpha \frac{\partial^2 T}{\partial y^2} + \frac{(\rho c)_{np}}{(\rho c)_{nf}} \left[D_B \frac{\partial c}{\partial y} \frac{\partial T}{\partial y} + \frac{D_T}{T_\infty} \left(\frac{\partial T}{\partial y} \right)^2 \right] \tag{3}$$

Concentration Equation:

$$u \frac{\partial c}{\partial x} + v \frac{\partial c}{\partial y} = D_B \frac{\partial^2 c}{\partial y^2} + \frac{D_T}{T_\infty} \left(\frac{\partial^2 T}{\partial y^2} \right) \tag{4}$$

with boundary conditions are

$$\begin{aligned} u &= U_w(x), v = -\delta(x), T = T_w, C = C_w \text{ at } y = 0, \\ u &= 0, T = T_\infty, C = C_\infty \text{ as } y \rightarrow \infty, \end{aligned} \tag{5}$$

we present the subsequent similarity transformations

$$\begin{cases} u = U_w f'(\eta), v = -(f'(\eta)\eta + f(\eta)) \left(\frac{\nu U_w}{2\ell} \right)^{1/2} \\ \eta = \gamma \left(\frac{U_w}{2\nu\ell} \right)^{1/2} y \\ T = -((T_\infty - T_w)g(\eta) - T_\infty), C = -((C_\infty - C_w)h(\eta) - C_\infty), \end{cases} \tag{6}$$

By using the above transformation, equations (2),(3) and (4) transforms PDE into following ODE problems

$$f''' + ff'' - 2f'^2 = 0 \tag{7}$$

$$g'' + g'(Ntg' + Nbh' + Prf) - f'g = 0 \tag{8}$$

$$h'' + NtNb^{-1}g'' - Le(hf' - fh') = 0 \tag{9}$$

$$\begin{aligned} f &= -v_w, f' = 1, g = 1, h = 1 \text{ at } \eta=0, \\ f' &\rightarrow 0, g \rightarrow 0, h \rightarrow 0 \text{ as } \eta \rightarrow \infty \end{aligned} \tag{10}$$

Where, $Nt = D_B \frac{(\rho c)_{np}}{(\rho c)_{nf}} (C_w - C_\infty)$, $Nb = \frac{D_T (\rho c)_{np} T_w - T_\infty}{T_\infty (\rho c)_{nf} v}$,
 $Le = \frac{v}{D_B}$, $Pr = \frac{v}{\alpha}$.

The physical significance of this problem is local skin friction coefficient, Nusselt number (Nu_x) and the Sherwood number (Sh_x) which are defined as

$$C_{fx} = \frac{T_w|_{y=0}}{\rho u_w^2}, Nu_x = -\frac{x}{T_w - T_\infty} \frac{\partial T}{\partial y} |_{y=0}, Sh_x = -\frac{x}{C_w - C_\infty} \frac{\partial C}{\partial y} |_{y=0}$$

$$(2Re)^{1/2} C_{fx} = f''(0), \frac{Nu_x}{(2Re_x)^{1/2}} = -\left(\frac{x}{2\ell}\right)^{1/2} g'(0),$$

$$\frac{Sh_x}{(2Re_x)^{1/2}} = -\left(\frac{x}{2\ell}\right)^{1/2} h'(0)$$

$Re = U_w \ell / v$ is the Reynolds number, and $Re_x = U_w x / v$ is the local Reynolds number.

III. VARIATIONAL HOMOTOPY PERTURBATION METHOD (VHPM)

As a means of elucidating the core principles underlying the modified variational iteration method, we can use the generic differential equation as an example.

$$Lu + Nu = h(x)$$

Here, $h(x)$ denotes the forcing term, L is a linear operator, N is a nonlinear operator, and we can construct a correction function using the variational method in the following manner. $u_{n+1}(x) = u_n(x) + \int_0^x \lambda(\mu) (Lu_n(\mu) + Nu_n(\mu) - h(\mu)) d\mu$

Where λ is a Lagrange multiplier. The subscript n denotes the n th approximation, and f is a restricted variation. The homotopy perturbation method is now used,

$$\sum_{n=0}^{\infty} p^n f_n = u_0(x)$$

$$= p \int_0^x \lambda(\mu) \left(\sum_{n=0}^{\infty} p^n L(u_n) + \sum_{n=0}^{\infty} p^n N(u_n) \right) d\mu - \int_0^x \lambda(\mu) h(\mu) d\mu,$$

Which is the variational iteration approach and Adomian's polynomials can be coupled to generate the variational homotopy perturbation method (VHPM). Solutions of varying orders can be found by comparing pairs of identical powers of p .

IV. SOLUTION OF VARIATIONAL HOMOTOPY PERTURBATION METHOD

For VHPM [23-26] solutions, the initial conditions are

$$f_0(\eta) = 1 - v_w - e^{-\eta}, g_0(\eta) = e^{-\eta}, h_0(\eta) = e^{-\eta}$$

To Solve the equations (7), (8) and (9) by using VHPM,

$$f_{n+1}(\eta) = f_n(\eta) + \int_0^\eta \lambda_1(\mu) \left(\frac{\partial^3 f_n(\mu)}{\partial \mu^3} - 2(\tilde{f}'_n(\mu))^2 + \tilde{f}_n(\mu) \tilde{f}''_n(\mu) \right) d\mu$$

$$g_{n+1}(\eta) = g_n(\eta) + \int_0^\eta \lambda_2(\mu) \left(\frac{\partial^2 g_n \mu}{\partial \mu} + Pr \left(\tilde{f}_n(\mu) \frac{\partial \tilde{g}_n(\mu)}{\partial \mu} - \tilde{g}_n(\mu) \frac{\partial \tilde{f}_n(\mu)}{\partial \mu} + Nb \frac{\partial \tilde{g}_n(\mu)}{\partial \mu} \frac{\partial \tilde{h}_n(\mu)}{\partial \mu} + Nt (\tilde{g}_n(\mu))^2 \right) \right) d\mu$$

$$h_{n+1}(\eta) = h(\eta) + \int_0^\eta \lambda_3(\mu) \left(\frac{\partial^2 h_n(\mu)}{\partial \mu^2} + Le \left(\tilde{f}_n(\mu) \frac{\partial \tilde{h}_n(\mu)}{\partial \mu} - \tilde{h}_n(\mu) \frac{\partial \tilde{f}_n(\mu)}{\partial \mu} + \frac{Nt}{Nb} \frac{\partial^2 g_n(\mu)}{\partial \mu^2} \right) \right) d\mu$$

The Lagrange multipliers are identified as,

$$\lambda_1(\mu) = -\frac{1}{2}(\mu - \eta)^2, \quad \lambda_2(\mu) = \lambda_3(\mu) = (\mu - \eta)$$

Consequently,

$$f_{n+1}(\eta) = f_n(\eta) - \frac{1}{2} \int_0^\eta (\mu - \eta)^2 \left(\frac{\partial^3 f_n(\mu)}{\partial \mu^3} - 2(\tilde{f}'_n(\mu))^2 + \tilde{f}_n(\mu) \tilde{f}''_n(\mu) \right) d\mu$$

$$g_{n+1}(\eta) = g_n(\eta) + \int_0^\eta (\mu - \eta) \left(\frac{\partial^2 g_n(\mu)}{\partial \mu^2} + Pr \left(\tilde{f}_n(\mu) \frac{\partial \tilde{g}_n(\mu)}{\partial \mu} - \tilde{g}_n(\mu) \frac{\partial \tilde{f}_n(\mu)}{\partial \mu} + Nb \frac{\partial \tilde{g}_n(\mu)}{\partial \mu} \frac{\partial \tilde{h}_n(\mu)}{\partial \mu} + Nt (\tilde{g}_n(\mu))^2 \right) \right) d\mu$$

$$h_{n+1}(\eta) = h_n(\eta) + \int_0^\eta (\mu - \eta) \left(\frac{\partial^2 h_n(\mu)}{\partial \mu^2} + Le \left(\tilde{f}_n(\mu) \frac{\partial \tilde{h}_n(\mu)}{\partial \mu} - \tilde{h}_n(\mu) \frac{\partial \tilde{f}_n(\mu)}{\partial \mu} + \frac{Nt}{Nb} \frac{\partial^2 g_n(\mu)}{\partial \mu^2} \right) \right) d\mu$$

Applying the VHPM, we get,

$$\begin{aligned}
 f_0 + pf_1 + \dots &= f_0(\eta) \\
 &- \frac{p}{2} \int_0^\eta (\mu - \eta)^2 \left(\left(\frac{\partial^3 f_0(\mu)}{\partial \mu^3} + p \frac{\partial^3 f_1(\mu)}{\partial \mu^3} \right. \right. \\
 &+ \dots \left. \left. - 2 \left(\frac{\partial f_0}{\partial \mu} + p \frac{\partial f_1}{\partial \mu} + \dots \right)^2 \right. \right. \\
 &+ (f_0 + pf_1 + \dots) \left(\frac{\partial^2 f_0(\mu)}{\partial \mu^2} + p \frac{\partial^2 f_1(\mu)}{\partial \mu^2} \right. \\
 &+ \dots \left. \left. \right) d\mu g_0 + pg_1 + \dots \\
 &= g_0(\eta) \\
 &+ \int_0^\eta (\mu \\
 &- \eta) \left(\left(\frac{\partial^2 g_0(\mu)}{\partial \mu^2} + p \frac{\partial^2 g_1(\mu)}{\partial \mu^2} + \dots \right) \right. \\
 &+ Pr \left((f_0(\mu) + pf_1(\mu) + \dots) \left(\frac{\partial g_0(\mu)}{\partial \mu} \right. \right. \\
 &+ p \frac{\partial g_1(\mu)}{\partial \mu} + \dots \left. \left. \right) \right. \\
 &- (g_0(\mu) + pg_1(\mu) + \dots) \left(\frac{\partial f_0(\mu)}{\partial \mu} \right. \\
 &+ p \frac{\partial f_1(\mu)}{\partial \mu} + \dots \left. \left. \right) \right. \\
 &+ Nb \left(\frac{\partial g_0(\mu)}{\partial \mu} + p \frac{\partial g_1(\mu)}{\partial \mu} + \dots \right) \left(\frac{\partial h_0(\mu)}{\partial \mu} \right. \\
 &+ p \frac{\partial h_1(\mu)}{\partial \mu} + \dots \left. \left. \right) \right. \\
 &+ Nt \left(\frac{\partial g_0(\mu)}{\partial \mu} + p \frac{\partial g_1(\mu)}{\partial \mu} + \dots \right)^2 \left. \right) d\mu
 \end{aligned}$$

$$\begin{aligned}
 h_0 + ph_1 + \dots &= h_0(\eta) \\
 &+ \int_0^\eta (\mu - \eta) \left(\frac{\partial^2 h_0(\mu)}{\partial \mu^2} + p \frac{\partial^2 h_1(\mu)}{\partial \mu^2} + \dots \right. \\
 &+ Le \left((f_0(\mu) + pf_1(\mu) + \dots) \left(\frac{\partial h_0(\mu)}{\partial \mu} \right. \right. \\
 &+ p \frac{\partial h_1(\mu)}{\partial \mu} + \dots \left. \left. \right) \right. \\
 &- (h_0(\mu) + ph_1(\mu) + \dots) \left(\frac{\partial f_0(\mu)}{\partial \mu} \right. \\
 &+ p \frac{\partial f_1(\mu)}{\partial \mu} + \dots \left. \left. \right) \right. \\
 &+ \frac{Nt}{Nb} \left(\frac{\partial^2 g_0(\mu)}{\partial \mu^2} + p \frac{\partial^2 g_1(\mu)}{\partial \mu^2} + \dots \right) \left. \right) d\mu
 \end{aligned}$$

Comparing the coefficient of like powers of p, we get

$$p^{(0)} = f_0(\eta) = 1 - v_w - e^{-\eta}$$

$$\begin{aligned}
 p^{(1)} = f_1(\eta) &= \frac{\eta}{1!} \left(\frac{1}{2} e^{-\eta} (1 - v_w) + \frac{3}{4} \right) \\
 &+ \frac{\eta^2}{2!} \left(\frac{1}{2} + (1 - v_w)(1 + e^{-\eta}) \right) - \frac{e^{-\eta} \eta^3}{3!} \\
 &- (1 - v_w)(1 - e^{-\eta}) - \frac{1}{4} (e^{-2\eta} - 1)
 \end{aligned}$$

The series solution is given by

$$\begin{aligned}
 f(\eta) &= \frac{\eta}{1!} \left(\frac{1}{2} e^{-\eta} (1 - v_w) + \frac{3}{4} \right) + \\
 &\frac{\eta^2}{2!} \left(\frac{1}{2} + (1 - v_w)(1 + e^{-\eta}) \right) - \frac{e^{-\eta} \eta^3}{3!} + e^{-\eta} ((1 - v_w) - \\
 &1) - \frac{1}{4} (e^{-2\eta} - 1) \quad (11)
 \end{aligned}$$

$$\begin{aligned}
 g(\eta) &= \frac{\eta}{1!} (Pr(1 - v_w)(2e^{-\eta} - 1)) - \frac{\eta^2}{2!} e^{-\eta} + \\
 Pr(1 - v_w)(e^{-\eta} - 1) - \frac{(Nb+Nt)}{4} (e^{-2\eta} + 1) + e^{-\eta} \quad (12)
 \end{aligned}$$

$$\begin{aligned}
 h(\theta) &= \frac{\eta}{1!} Le(1 - v_w) - \frac{\eta^2}{2!} e^{-\eta} \left(1 + \frac{Nt}{Nb} \right) + Le(1 - \\
 v_w)(e^{-\eta} - 1) + e^{-\eta} \quad (13)
 \end{aligned}$$

Numerical Process

The numerical solution of equations (7), (8) & (9) are satisfies the boundary conditions equation (10)

$$\begin{aligned}
 f = y(1), f' = y(2), f'' = y(3), g = y(4), g' = y(5), \\
 h = y(6), h' = y
 \end{aligned}$$

Rearrange the equation (7) to (9)

$$\begin{aligned}
 f''' &= -ff'' + 2f'^2 \\
 g'' &= -g'(Ntg' + Nbh' + Prf) + f'g \\
 h'' &= -NtNb^{-1}g'' + Le(hf' - fh')
 \end{aligned}$$

$$\begin{aligned}
 Bcs, ya(1) - vw, ya(2) = 1, yb(2) = 0, ya(4) \\
 = 1, ya(6) = 1
 \end{aligned}$$

Velocity Profile:

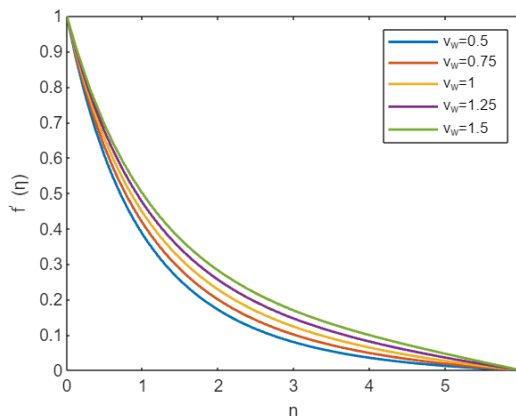


Figure 2: Effects of the v_w in the velocity profile

Temperature Profile:

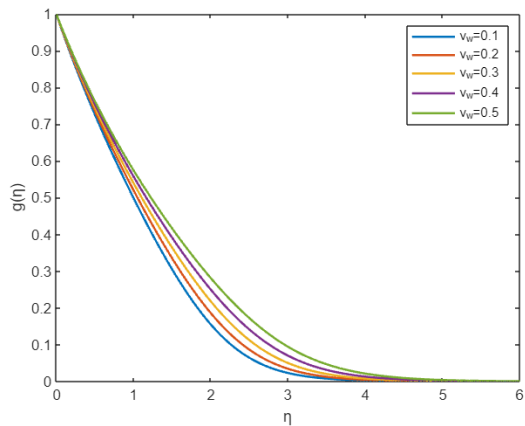


Figure 3: Effects of v_w , on $Pr = 3, Nb = 0.5, Nt = 1.5, Le = 1$.

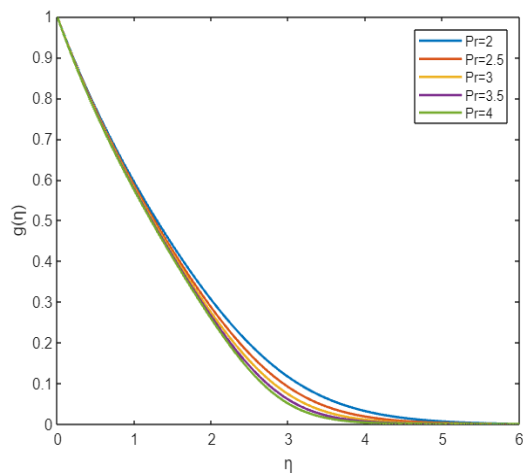


Figure 6: Effects of Pr on $Nb = 0.5, Nt = 2, Le = 1, v_w = 0.25$

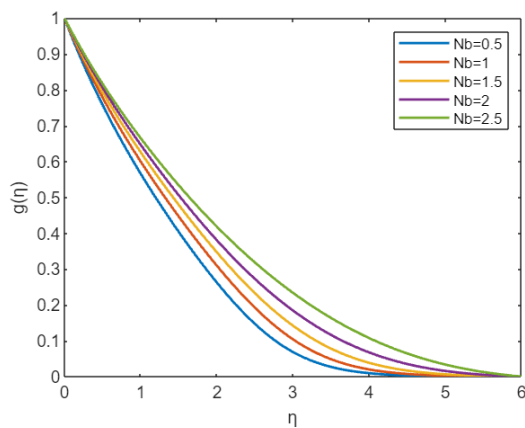


Figure 4: Effects of Nb , on $Pr = 4, Nt = 1.5, Le = 1, v_w = 0.5$

Concentration Profile:

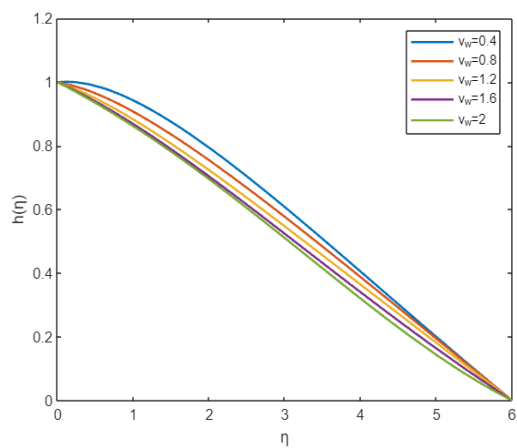


Figure 7: Effects of v_w , on $Pr = 0.7, Nb = Nt = 0.5, Le = 0.2$

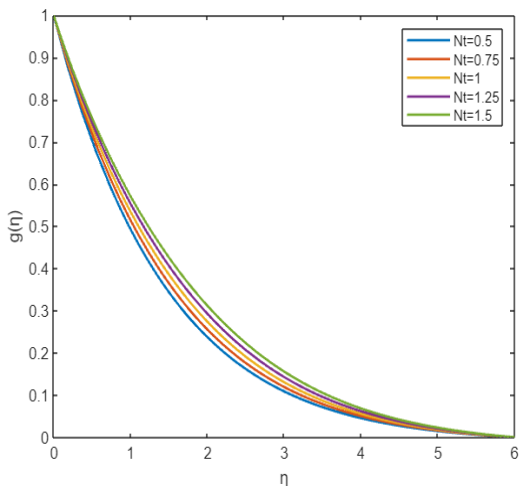


Figure 5: Effects of Nt , on $Pr = 1, Le = 1, Nb = 0.01, v_w = 0.25$

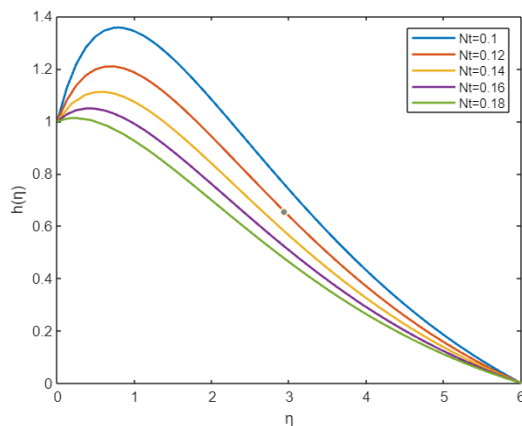


Figure 8: Effects of Nt , on $Pr = 0.7, Nb = 0.5, Le = 1, v_w = 0.2$

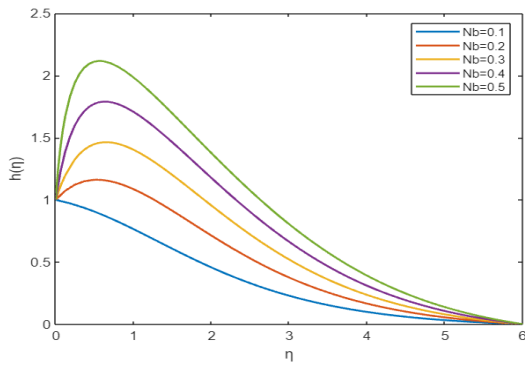


Figure 9: Effects of Nb , on $Pr = 2$, $Nt = 0.1$, $Le = 1$, $v_w = 0.2$

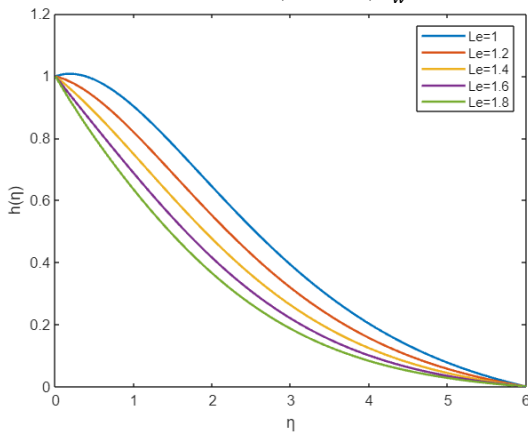


Figure 10: Effects of Le , on $Pr = 1$, $Nb = 0.2$, $Nt = 0.1$, $v_w = 0.2$

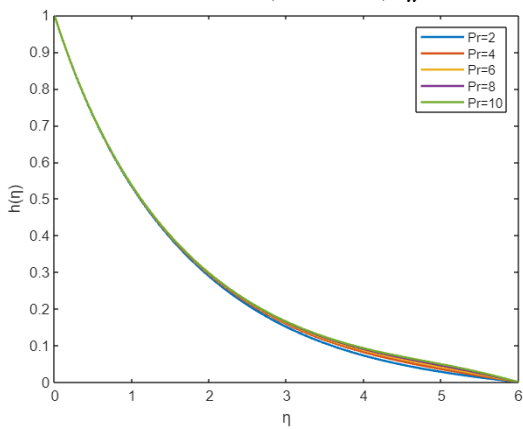


Figure 11: Effects of Pr , on $Nb = 0.5$, $Le = Nt = 2$, $v_w = 1$

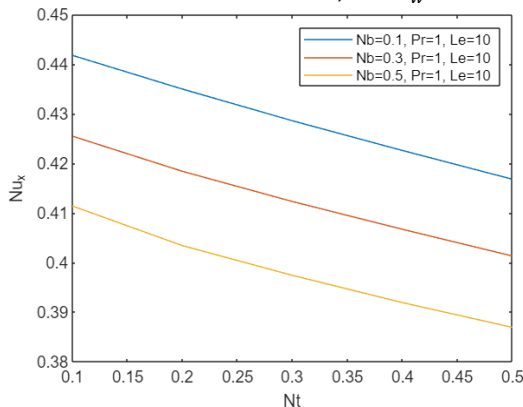


Figure 12: Effects of Nt on heat transfer coefficient

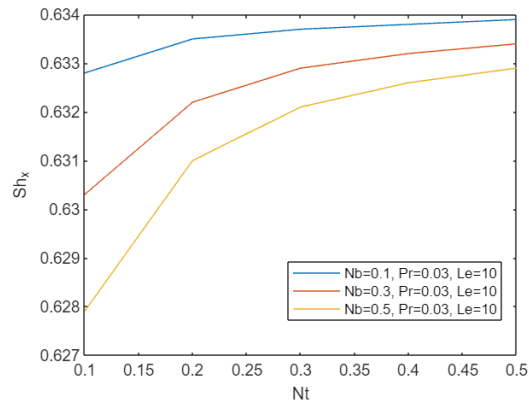


Figure 13: Effects Nb on mass transfer coefficient at $Le = 10$

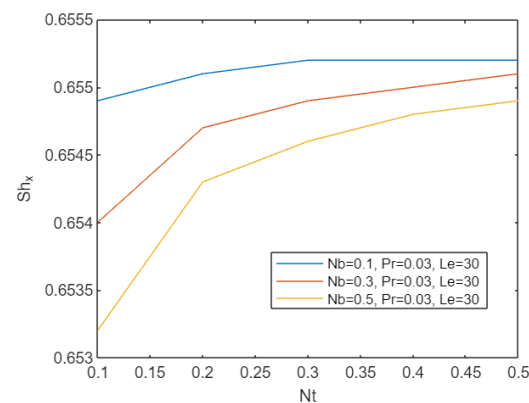


Figure 14: Effects of Nt on mass transfer coefficient $Le = 30$

Table. 1. Comparison values of reduced Nu_x and Sh_x for various Pr values

Pr	Makinde & Aziz [32]		Present results	
	Nu_x	Sh_x	Nu_x	Sh_x
1	0.0789	1.5477	0.0789	1.5477
2	0.0806	1.5554	0.0806	1.5554
5	0.0735	1.5983	0.0735	1.5983

V. RESULTS AND DISCUSSION

In the present section, we examine the 2D laminar boundary layer flow of nanoliquid over an exponential SS. The transformed ODE's equations (7) – (9) are solved numerically by using bvp4c method. The effects of physical parameters for momentum, heat and mass profiles such as Lewis number (Le), Brownian motion parameter (Nb), thermophoresis parameter (Nt), Prandtl number (Pr), suction and injection parameter (v_w). As depicted in Figure (2), the acceleration increases when enhancing the suction or injection parameter.

The effects of suction or injection (v_w), Brownian motion (Nb), thermophoresis (Nt) parameters and Prandtl number (Pr) on temperature profiles are portrayed in Figure (3) – (6). In figure. 3, It is observed that the hotness of the liquid

enhances due to the higher range of the suction or injection (v_w). Figure 4 and 5 illustrate, respectively, the impact of Nb and the Nt on the temperature profile. In this situation, temperature is a function that grows as a function of both constants. The temperature has to go up in order to see an improvement in these factors. The Nb is responsible for the generation of micro-mixing, which in turn improves the thermal performance of the base liquid. In addition, the Nb of nanoparticles is a process of nanotechnology guiding their thermal performance at both the nanoscale and the molecular stage. Nb occurs when determining the classification of nanofluids based on the size of the nanoparticles, which can have an effect on the parameters of heat transfer. When the sizes of the particles tend towards the nanoscale scale, Brownian motion of the particles and its impact on liquids in the surrounding area play a significant role in the transmission of heat. whereas it declines the Prandtl number. Physically, the decrease in the temperature profile is a consequence of a fact that, as the Prandtl number improves thermal diffusivity reduces (See Figure. 6).

Figure (7) – (11) draws the consequences of suction or injection (v_w), Brownian motion (Nb), thermophoresis (Nt) parameters and Lewis number (Le) on concentration profile ($h(\eta)$). From Figure.7 it is noticed that the $h(\eta)$ enhances for the rise in suction or injection parameter (v_w). Figures 8 and 9 depict, respectively, the effect of Nt and Nb on the $h(\eta)$. As depicted in these graphs, nanofluid constants exert opposite effects on the nanoparticle volume fraction profile. By increasing the Nt , the concentration of nanoparticles and their associated boundary thickness increase. However, as the rate of Nb increases, the $h(\eta)$ values tend to decrease. Physically, an increase in the Nt constant results in an increase in the Nt energy, which indicates that nanoparticles are moving from heated to cold areas; consequently, the nanoparticle volume fraction increases. In addition, increasing the Nb reduces nanoparticle diffusion into the liquid regime away from the surface; consequently, the $h(\eta)$ in the boundary layer decreases.

Figure 10 and 11 shows the enhancement in $h(\eta)$ for higher values of Prandtl number (Pr) and Lewis number (Le). Physically, particles are accelerated away from the field zone and the liquid in the boundary layer is warmed due to the Brownian motion. Thus, the concentration is shown to decrease. The contrast between the local Nusselt number for (Nt) is depicted in Figure. 12, It is uncovered that the HT decrease when the values of Nusselt number increases. Figure (13) – (14) shows the consequences of Sherwood number for different values of Lewis number ($Le = 10$ & 30) in Nt . From this figure it is seen that the mass transfer decrease when the values of Nt increases. Table. 1 compares the Nusselt number and Sherwood number current flow with the earlier reference [32], which we observed in a unique validation.

VI. CONCLUSION

Examining the impact of Brownian motion and thermophoresis on the heat transfer (HT) in the boundary layer was essential for analysing the laminar two-dimensional boundary layer flow of a nanoliquid past an exponentially SS. The following is a concise summary of the results of the analysis. An increase in the suction

parameters causes an increase in the fluid flow; nevertheless, an enhancement in the suction parameters also has a rising tendency to raise the temperature and concentration profiles. Both Nt and Nb constants exhibit an opposite effect on the concentration as well as the mass transfer rate. Intensifying the Nt has a positive effect on the concentration as well as the thermal and boundary layer thicknesses.

REFERENCES

- [1] Choi, S.U.S., Eastman, J.A. "Enhancing thermal conductivity of fluids with nanoparticle, Developments and Applications of Non-Newtonian Flows." In Proceedings of the ASME International Mechanical Engineering Congress and Exhibition, San Francisco, CA, USA, 12–17 November 1995; Volume 231, pp. 99–105.
- [2] Jalili, B., Emad, M., Jalili, P., Ganji, D.D., Saleem, S. and Tag-eldin, E.M. "Thermal analysis of boundary layer nanofluid flow over the movable plate with internal heat generation, radiation, and viscous dissipation." Case Studies in Thermal Engineering, 2023, pp.103203.
- [3] Patil, P.M., Hiremath, P.S. and Momoniati, E. "Impulsive motion causes time-dependent nonlinear convective Williamson nanofluid flow across a rough conical surface: Semi-similar analysis." Alexandria Engineering Journal, 74, 2023, pp.171-185.
- [4] Mahesh, R., Mahabaleshwar, U.S., Kumar, P.V., Oztop, H.F. and Abu-Hamdeh, N. "Impact of radiation on the MHD couple stress hybrid nanofluid flow over a porous sheet with viscous dissipation." Results in Engineering, 17, 2023, pp.100905.
- [5] Alzahrani, A.K., Ullah, M.Z., Alshomrani, A.S. and Gul, T. "Hybrid nanofluid flow in a Darcy-Forchheimer permeable medium over a flat plate due to solar radiation." Case Studies in Thermal Engineering, 26, 2021, pp.100955.
- [6] Rauf, A., Hussain, F., Mushtaq, A., Shah, N.A. and Ali, M.R. "MHD mixed convection flow for Maxwell Hybrid nanofluid with Soret, Dufour and Morphology effects." Arabian Journal of Chemistry, 16(8), 2023, pp.104965.
- [7] Rawat, S.K., Yaseen, M., Shafiq, A., Kumar, M. and Al-Mdallal, Q.M. "Nanoparticle aggregation effect on nonlinear convective nanofluid flow over a stretched surface with linear and exponential heat source/sink." International Journal of Thermofluids, 2023, pp.100355.
- [8] Verma, A.K., Rajput, S., Bhattacharyya, K. and Chamkha, A.J. "Nanoparticle's radius effect on unsteady mixed convective copper-water nanofluid flow over an expanding sheet in porous medium with boundary slip." Chemical Engineering Journal Advances, 12, 2022, pp.100366.
- [9] Wang, F., Awais, M., Parveen, R., Alam, M.K., Rehman, S. and Shah, N.A. "Melting rheology of three-dimensional Maxwell nanofluid (Graphene-Engine-Oil) flow with slip condition past a stretching surface through Darcy-Forchheimer medium." Results in Physics, 2023, pp.106647.
- [10] Amjad, M., Khan, M.N., Ahmed, K., Ahmed, I., Akbar, T. and Eldin, S.M. "Magnetohydrodynamics tangent hyperbolic nanofluid flow over an exponentially stretching sheet: Numerical investigation." Case Studies in Thermal Engineering, 45, 2023, pp.102900.
- [11] Jawad, M., Hameed, M.K., Nisar, K.S. and Majeed, A.H., 2023. "Darcy-Forchheimer flow of maxwell nanofluid flow over a porous stretching sheet with Arrhenius activation energy and nield boundary conditions." Case Studies in Thermal Engineering, 44, pp.102830.
- [12] Alrehili, M. "Improvement for engineering applications through a dissipative Carreau nanofluid fluid flow due to a nonlinearly stretching sheet with thermal radiation." Case Studies in Thermal Engineering, 42, 2023, pp.102768.
- [13] Eswaramoorthi, S., Divya, S., Faisal, M. and Namgyel, N. "Entropy and heat transfer analysis for MHD flow of Cu/Ag-water-based nanofluid on a heated 3D plate with nonlinear radiation." Mathematical Problems in Engineering, 2022, 2022, pp.1-14.
- [14] Negi, A.S., Kumar, A., Yaseen, M., Rawat, S.K. and Saini, A. "Effects of heat source on the stagnation point flow of a nanofluid over a stretchable sheet with magnetic field and zero mass flux at the surface." Forces in Mechanics, 11, 2023, pp.100190.
- [15] Sedki, A.M. "Effect of thermal radiation and chemical reaction on MHD mixed convective heat and mass transfer in nanofluid flow due to nonlinear stretching surface through porous medium." Results in Materials, 16, 2022, pp.100334.

- [16] Alrehili, M. "Viscoelastic thermal nanofluid flow and heat mass transfer due to a stretching sheet with slip velocity phenomenon and convective heating." *International Journal of Thermofluids*, 2023, pp.100281.
- [17] Shatanawi, W., Abbas, N., Shatnawi, T.A. and Hasan, F. "Heat and mass transfer of generalized fourier and Fick's law for second-grade fluid flow at slendering vertical Riga sheet." *Heliyon*, 9(3), 2023.
- [18] Saidulu, B. and Reddy, K.S. "Evaluation of combined heat and mass transfer in hydromagnetic micropolar flow along a stretching sheet when viscous dissipation and chemical reaction is present." *Partial Differential Equations in Applied Mathematics*, 7, 2023, pp.100467.
- [19] Guled, C.N., Tawade, J.V., Kumam, P., Noeiaghdam, S., Maharudrappa, I., Chithra, S.M. and Govindan, V. "The heat transfer effects of MHD slip flow with suction and injection and radiation over a shrinking sheet by optimal homotopy analysis method." *Results in Engineering*, 18, 2023, pp.101173.
- [20] Loganathan, K., Eswaramoorthi, S., Chinnasamy, P., Jain, R., Sivasakthivel, R., Ali, R. and Devi, N.N. Heat and Mass Transport in Casson Nanofluid Flow over a 3-D Riga Plate with Cattaneo-Christov Double Flux: A Computational Modeling through Analytical Method. *Symmetry*, 15(3), 2023, pp.725.
- [21] Divya, S., Eswaramoorthi, S. and Loganathan, K. "Numerical computation of Ag/Al₂O₃ nanofluid over a Riga plate with heat sink/source and non-Fourier heat flux model." *Mathematical and Computational Applications*, 28(1), 2023, pp.20.
- [22] Eswaramoorthi, S., Alessa, N., Sangeethavaanee, M., Kayikci, S. and Namgyel, N. "Mixed Convection and Thermally Radiative Flow of MHD Williamson Nanofluid with Arrhenius Activation Energy and Cattaneo-Christov Heat-Mass Flux." *Journal of Mathematics*, 2021, 2021, pp.1-16.
- [23] Amruta Daga, Vikas Pradhan "Variational Homotopy Perturbation method for the nonlinear Generalized Regularized long wave Equation." *American Journal of Applied Mathematics and Statistics*, 2014, 2(4).
- [24] O.Abdulaziz, ishk Hashim , M.S.H .Chowdhury "Solving Variational problems by homotopy perturbation method." *International Journal for Numerical methods in Engineering*, 2008, 75(6):709-721.
- [25] Francisco M. Fernandez, "On the Variational homotopy perturbation method for nonlinear Oscillators", *Journal of Mathematical physics*, 2012, 53 (2), 024101.
- [26] Muhammad Aslam Noor, Syed Tauseef Mohyud-Din, "Variational Homotopy Perturbation Method for Solving Higher Dimensional Initial Boundary Value Problems", *Mathematical Problems in Engineering*, 2008, vol. 2008, 696734.
- [27] Devaki B, Sampath Kumar V S, and Nityananda P Pai, "Analysis of Casson Flow Through Parallel and Uniformly Porous Walls of Different Permeability," *IAENG International Journal of Applied Mathematics*, vol. 53, no.1, pp9-16, 2023.
- [28] Selvi R. and Shukla P. "Analytical Solutions of Non-Newtonian Fluid through a Reiner-Rivlin Liquid Sphere with Cell Surface," *IAENG International Journal of Applied Mathematics*, vol. 52, no.4, pp811-816, 2022.
- [29] Gandhimathi T, Eswaramoorthi S, Loganathan K, Mishra NK, "Mathematical Modeling of MHD Flow of CNTs/Ag Nanoparticles Past a Heated Stretchy Surface with Nonuniform Heat Sink/Source and Thermal Radiation Impacts", *Mathematical Problems in Engineering*, vol. 2023, Article ID 7308650, 18 pages, 2023.
- [30] Fawzia Mansour Elniel, Shaymaa Mustafa, Arifah Bahar, Zainal Abdul Aziz, and Faisal Salah, "Effects of Shear Stress on Magnetohydrodynamic (MHD) Powell Eyring Fluid over A Porous Plate: A Lift and Drainage Problem," *IAENG International Journal of Applied Mathematics*, vol. 51, no.4, pp851-860, 2021.
- [31] Mahalakshmi D, Vennila B; "Boundary layer flow of silver and gold nanofluids over a flat plate by adomain decomposition method". *AIP Conference Proceedings* 6 November 2020; 2277 (1): 170002.
- [32] Makinde OD, Aziz A, "Boundary layer flow of a nanofluid past a stretching sheet with a convective boundary condition", *Int. J. Therm. Sci.* 2011: 50;1326-1332.

First author D. Mahalakshmi also works as an Assistant Professor in the Department of Mathematics, SRM Arts and Science College, SRM Nagar, Kattankulathur, Chengalpattu-603 203, Tamil Nadu, India.